A nonRD receptor-like kinase prevents nodule early senescence and defense-like reactions during symbiosis

Fathi Berrabah, Marie Bourcy, Alexis Eschstruth, Anne Cayrel, Ibtissem Guefrachi, Peter Mergaert, Jiangqi Wen, Viviane Jean, Kirankumar Mysore, Benjamin Gourion, et al.

New Phytologist

Research

A nonRD receptor-like kinase prevents nodule early senescence and defense-like reactions during symbiosis

Fathi Berrabah[1], Marie Bourcy[1], Alexis Eschstruth[1], Anne Cayrel[1], Ibtissem Guefrachi[1], Peter Mergaert[1], Jiangqi Wen[2], Viviane Jean[1], Kirankumar S. Mysore[2], Benjamin Gourion[1]* and Pascal Ratet[1]*

[1]Institut des sciences du végétal, CNRS, Saclay Plant Sciences, Avenue de la terrasse, 91198, Gif Sur Yvette, France; [2]Plant Biology Division, The Samuel Roberts Noble Foundation, 2510 Sam Noble Parkway, Ardmore, OK 73401, USA

Authors for correspondence:
Benjamin Gourion
Tel: +33 1 6982 3574
Email: benjamin.gourion@isv.cnrs-gif.fr

Pascal Ratet
Tel: +33 1 6982 3574
Email: pascal.ratet@isv.cnrs-gif.fr

Received: *17 March 2014*
Accepted: *30 April 2014*

New Phytologist (2014) **203:** 1305–1314
doi: 10.1111/nph.12881

Key words: chronic infection, defense reactions, endosymbiosis, intracellular infection, nitrogen fixation, nodulation, rhizobium.

Summary

- Rhizobia and legumes establish symbiotic interactions leading to the production of root nodules, in which bacteria fix atmospheric nitrogen for the plant's benefit. This symbiosis is efficient because of the high rhizobia population within nodules. Here, we investigated how legumes accommodate such bacterial colonization.
- We used a reverse genetic approach to identify a *Medicago truncatula* gene, *SymCRK*, which encodes a cysteine-rich receptor-like kinase that is required for rhizobia maintenance within the plant cells, and performed detailed phenotypic analyses of the corresponding mutant.
- The *Medicago truncatula symCRK* mutant developed nonfunctional and necrotic nodules. A nonarginine asparate (nonRD) motif, typical of receptors involved in innate immunity, is present in the SymCRK kinase domain. Similar to the *dnf2* mutant, bacteroid differentiation defect, defense-like reactions and early senescence were observed in the *symCRK* nodules. However, the *dnf2* and *symCRK* nodules differ by their degree of colonization, which is higher in *symCRK*. Furthermore, in contrast to *dnf2*, *symCRK* is not a conditional mutant.
- These results suggest that in *M. truncatula* at least two genes are involved in the symbiotic control of immunity. Furthermore, phenotype differences between the two mutants suggest that two distinct molecular mechanisms control suppression of plant immunity during nodulation.

Introduction

Legumes and rhizobia establish symbiotic interactions that result in the formation of root organs (the nodules) housing bacteria that fix atmospheric nitrogen for the benefit of the plant (Oldroyd *et al.*, 2011; Udvardi & Poole, 2013). The symbiosis is efficient as a result of the chronic and massive bacterial invasion of the nodule cells. Despite the massive colonization of their tissues, plants do not develop defense reactions in response to the endosymbionts (bacteroids) (Berrabah *et al.*, 2014). The relationship between immunity and symbiosis has been investigated before, but the majority of these studies focused on the early step of the symbiosis, that is, the infection process (Zamioudis & Pieterse, 2012). How plants tolerate massive intracellular invasion in the symbiotic organ remains poorly documented (Zamioudis & Pieterse, 2012; Bourcy *et al.*, 2013a). However, deciphering this mechanism is a necessity for the potential transfer of the nitrogen-fixing symbiotic capacity to nonlegume plants, which is currently a challenge (Charpentier & Oldroyd, 2010; Beatty & Good, 2011). In addition, understanding how eukaryotes can accommodate such massive intracellular infection by a foreign organism might also have impacts on other fundamental biological questions such as the evolutionary acquisition of endosymbionts, as well as the maintenance of intracellular pathogenic bacteria.

The recently released genome sequence (Young *et al.*, 2011), the accumulation of transcriptomics data gathered in a gene expression atlas (Benedito *et al.*, 2008; He *et al.*, 2009) and the existence of large collections of tagged mutants (Tadege *et al.*, 2008; Iantcheva *et al.*, 2009; Cheng *et al.*, 2011) with an increasing number of available flanking sequence tags (FSTs; http://bioinfo4.noble.org/mutant/database.php) make *Medicago truncatula* one of the favorite models to study rhizobium–legume interactions. In *M. truncatula*, nodules have a persistent meristem in the apical region, referred to as zone I, which is separated from zone III, in which bacteria fix nitrogen, by zone II, in which bacteria invade plant cells (Vasse *et al.*, 1990). In zone III of *M. truncatula* nodules, the infected cells produce nodule-specific cysteine-rich (NCR) antimicrobial peptides that trigger the terminal differentiation of bacteroids (Van de Velde *et al.*, 2010). As a consequence of the action of these peptides, the bacteroids are elongated and become polyploid (Kondorosi *et al.*, 2013). In parallel, in zone III, the plant nuclei undergo endoreduplication, resulting in an endoploidy level up to 64C (Maunoury *et al.*, 2010). Nodule aging causes the development of a fourth zone (IV) in which both bacteria and plant cells senesce (Vasse *et al.*, 1990).

*These authors contributed equally to the work.

We recently described the *DNF2* gene that is required for bacteroid differentiation and persistence in *M. truncatula* (Bourcy *et al.*, 2013b). The nodules of the *dnf2* mutant display typical traits, suggesting defense-like reactions such as the induction of defense genes, the accumulation of phenolic compounds and the death of the symbiotic partner (Bourcy *et al.*, 2013a,b; Berrabah *et al.*, 2014). *DNF2* encodes a nodule-specific phosphatidylinositol phospholipase C X domain containing protein, but the link between plant defense repression and the biochemical activity of DNF2 has not yet been described. To get deeper insight into symbiotic control of plant immunity, we searched for *DNF2* coexpressed genes and report here the discovery of a second gene required to suppress plant defense-like reactions in nodules.

Materials and Methods

Plant and bacterial cultures

Except when explicitly mentioned, *Medicago truncatula* Gaertn ecotypes R108 (Hoffmann *et al.*, 1997) and its corresponding mutants *dnf2–4* (Pislariu *et al.*, 2012; Bourcy *et al.*, 2013b), and all mutants described in Supporting Information Table S1 were cultivated *in vitro* on buffered nodulation medium (BNM) (Ehrhardt *et al.*, 1992) solidified with 2% bacto-agar. Phytagel (0.8%) was also used as an alternative solidifying agent. For flow cytometry material preparation, plants were cultivated in growth chamber on a mixture of perlite and sand (1/2, v/v). *Sinorhizobium meliloti* strain Rm41 (Kondorosi *et al.*, 1984), strain 1021 WT (Galibert *et al.*, 2001), strain 1021 *bacA* (Ferguson *et al.*, 2002) and strain 2011 (Rosenberg *et al.*, 1981), as well as *S. medicae* strain WSM419 (Howieson & Ewing, 1986), were cultivated in yeast extract broth (YEB) medium (Krall *et al.*, 2002). The strain used for each experiment is indicated in the corresponding figure legend.

Complementation experiment

SymCRK, including its 4 kbp upstream region corresponding to the putative promoter region, was amplified using primers BG44 5′-CACCGAGATTGTGGCATCAGCTTATCC-3′ and MtRec3 5′-TATGACAACAACTTAAAACCTTGTCA-3′, cloned into the pENTR/D-Topo (Invitrogen) and transferred to pK7WG. *Agrobacterium rhizogenes* strain Arqua1 was used to transform the root system of *symCRK* mutant (NF0737). Hairy root transformation was performed as described earlier (Boisson-Dernier *et al.*, 2001). Briefly, after germination, plantlet root tips were removed using a scalpel and the cut roots were soaked in an *A. rhizogenes* suspension. Plants were then grown on BNM solid medium containing kanamycin.

Identification of the *PLA2* mutant

Polymerase chain reaction screening was performed as described in (Tadege *et al.*, 2008; Cheng *et al.*, 2011, 2013) using *PLA2*-specific primers PLA2a 5′-CCACAAAAATGCTTCCAGTACTTGT-3′ and PLA2b 5′-CCTTGTTAATTTCTTGAAAATACCA-3′.

Acetylene reduction assay

Acetylene reduction assay (ARA) was conducted on individual plants with a protocol modified from Koch & Evans (1966). Briefly, 14 d after inoculation, individual whole plants were placed into 10 ml glass vials sealed with rubber septa. Acetylene (250 µl) was injected into each vial. Gas samples (200 µl) were withdrawn after at least 1 h incubation at room temperature and the ethylene that was produced was measured by GC. The assay was done in triplicate.

SymCRK cDNA cloning

SymCRK cDNA was cloned into PEntr/D-Topo after amplification from cDNAs prepared from R108 nodules using primers BG54 5′-caccATGGCTTACAATCTGAAACAAAAACTG-3′ and MtRec3 5′-TATGACAACAACTTAAAACCTTGTCA -3′ and sequenced.

RT-qPCR

RNA extraction, cDNA synthesis and reverse transcription quantitative polymerase chain reaction (RT-qPCR) were performed as previously described (Bourcy *et al.*, 2013b). The primers used in this study are listed in Table S2 and have been described previously (Gao *et al.*, 2007; Samac *et al.*, 2011; Nars *et al.*, 2013).

Microscopy

Semithin sections (7 µm) of nodules were prepared as previously described (Van de Velde *et al.*, 2006). For the live/dead staining procedure, nodule sections were stained, prepared and observed as previously described (Haag *et al.*, 2011; Bourcy *et al.*, 2013b). Phenolic compounds were stained using potassium permanganate and methylene blue (Vasse *et al.*, 1993) and observed as previously described (Bourcy *et al.*, 2013b).

Flow cytometry analysis

Bacteroid material preparation and analysis were essentially conducted as described by Mergaert *et al.* (2006). Briefly, bacteroids were extracted from nodules 35 d after inoculation. Nodules were homogenized in a mortar and pestle with an ice-cold bacteroid extraction buffer (BEB; 125 mM KCl, 50 mM Na-succinate, 50 mM N-[Tris(hydroxymethyl)methyl]-2-aminoethanesulfonic acid sodium salt (TES) buffer, pH 7, 1% BSA). In order to eliminate debris, homogenates were centrifuged three times at 100 ***g*** at 18°C for 10 min and supernatants containing bacteroids were collected and centrifuged at 2000 ***g*** for 10 min. Bacteroid pellets were resuspended in 100 µl of BEB, and heated at 70°C for 10 min. Bacteroids were stained with 50 µg ml^{-1} 4′,6′-diamidino-2-phenylindol (DAPI). Measurements were performed with a Beckman-Coulter (Danvers, MA, USA) ELITE ESP flow cytometer. For nuclei preparation, 35-d-old nodules were treated as described by Mergaert *et al.* (2006).

Results

Identification of *DNF2* coregulated genes as candidates for repression of plant immunity during the symbiotic process

In order to identify new genes potentially involved in the control of plant defenses during symbiosis, we searched for *DNF2* coregulated genes, hypothesizing that some of them might be involved in plant immunity suppression. The *M. truncatula* gene expression atlas (MtGEA) was used for this purpose. Based on predicted function and on Pearson correlation coefficient calculated from expression data, three candidate genes were selected. These genes are annotated as a phospholipase A2 (*PLA2*), a sterol 3-β-glucosyltransferase and a cysteine-rich receptor-like kinase (*CR RLK*, Fig. 1) whose expression profile had the highest similarity with *DNF2* (Fig. S1). Table S1 describes the Pearson correlation for the three candidate genes. *Tnt1*-tagged mutant lines with *Tnt1* insertion in these genes were identified from the Noble Foundation *M. truncatula* mutant collection (http://bioinfo4.noble.org/mutant/database.php; Table S1, Fig. S1; Tadege *et al.*, 2008). Mutant lines harboring insertions in *CR RLK* (NF0737) and in the sterol 3-β-glucosyltransferase gene (NF4831) were identified by searching the FST database, while the mutant with insertion in *PLA2* (NF6259) was identified by PCR-based reverse screening as previously described (Cheng *et al.*, 2013). In order to determine if the *Tnt1* insertion in these genes alters nodule development and symbiosis, segregation analysis was performed on the T2 offspring of the mutant lines. Heterozygous, homozygous mutant or wild-type-like plants at the candidate loci were selected from the progenies of these lines (Table S3) and then tested for their capacity to establish symbiosis *in vitro*. Based on nodule pigmentation, only plants with insertion in the *CR RLK* locus and originating from the line NF0737 showed a defect in the symbiotic process and did not produce typical pink-colored functional nodules (Table S3, Fig 2b). Mutants with insertions in the other two genes, sterol 3-β-glucosyltransferase and *PLA2*, did not show symbiotic defects. Plants homozygous for insertion at the *CR RLK* locus had progenies with only white or necrotic nodules (Table S3). By contrast, progenies of a plant heterozygous for insertion at the *CR RLK* locus segregated as plants with wild-type nodules (19 plants) and plants with necrotic nodules (nine plants; Table S3), suggesting a strong link between the nodule phenotype and the mutation. In order to prove the

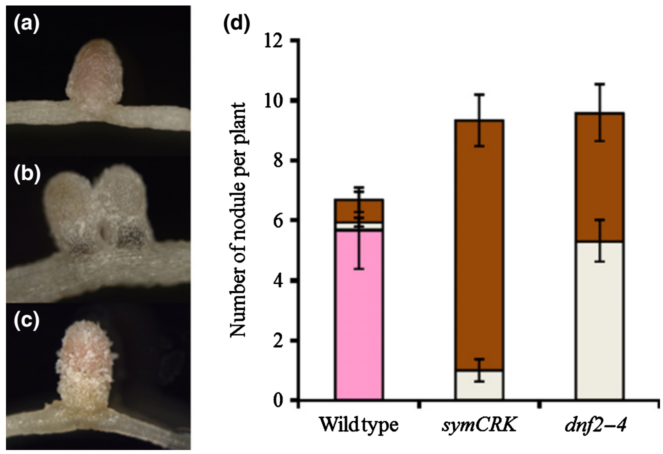

Fig. 2 SymCRK prevents nodule necrosis. (a–c) Nodules induced by *Sinorhizobium meliloti* Rm41 on *Medicago truncatula* wild-type (a), or on hairy roots of the NF0737 mutant line homozygous for *SymCRK* insertion (b, c), transformed with a control vector (b) or with a complementation vector (c). (d) The number of white (white bars), pink (pink bars) and necrotic (brownish) nodules produced per plant ($n = 15$) by the wild-type, the NF0737 and the *dnf2–4* lines. Error bars, ± SE. A chi-squared test of homogeneity indicates that proportions of white and brownish nodules are different for *dnf2–4* and *symCRK* (value of the test for one degree of freedom: 3.6×10^{-16}). This experiment has been reproduced with similar results.

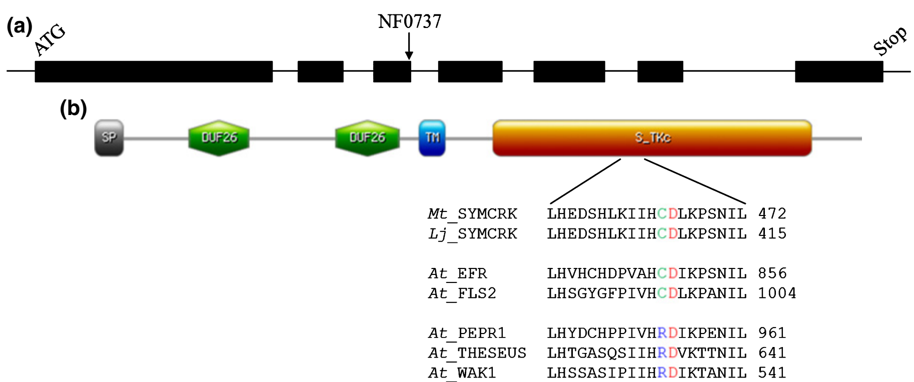

Fig. 1 SymCRK is a member of the nonarginine asparate (nonRD) kinase family. (a) The *SymCRK* gene structure; *SymCRK* has seven exons (black boxes) and six introns (2839 bp from ATG to Stop). The position of the *Tnt1* insertion disrupting the third exon of *SymCRK* in the NF0737 line (1065 bp downstream the ATG) is indicated by an arrow. (b) The predicted protein domains. A predicted signal peptide is present on the N-terminal (SP), followed by two cysteine-rich domains of unknown function (DUF26), a transmembrane domain and a serine/threonine protein kinase domain. The activation loop of the protein kinase domain harbors a nonRD motif represented by a green C and a red D. This motif is typical of pattern recognition receptor such as *At*_EFR and *At*_FLS2 and is not present in most kinases, such as *At*_PEPR1, *At*_THESEUS and *At*_WAK1, which harbor an RD motif represented by a blue R and a red D.

requirement of *CR RLK* for the symbiotic process, the gene was cloned with its native promoter region (i.e. ~ 4 kbp upstream of the predicted start codon) and was expressed using hairy root transformation in NF0737 roots. In contrast to the NF0737 line that displayed white or necrotic nodules, the complemented root systems produced pink nodules similar to that of the wild-type R108 (Fig. 2b,c). Unambiguously, these results indicate that the *CR RLK* is required for the symbiotic process. For these reasons, we named this gene *M. truncatula* Symbiotic CR RLK (*Mt_SymCRK*).

SymCRK encodes a nodule-specific receptor-like kinase of the nonarginine aspartate (nonRD) family

The microarray data from the MtGEA suggested that the *SymCRK* gene is exclusively expressed in nodules but not in other plant tissues subjected to various physiological conditions included in the database (Fig. S1). However, the MtGEA dataset was mainly constructed with the *M. truncatula* ecotype Jemalong A17, while the NF0737 mutant is in the R108 ecotype. In order to determine whether the *SymCRK* gene is also specifically expressed in nodules of the *M. truncatula* R108 ecotype, RT-qPCR experiments were performed using RNA isolated from leaves, stems, petioles, roots, and nodules. In agreement with the data obtained with *M. truncatula* Jemalong, in the R108 background, the expression of *Mt_SymCRK* was detectable only in nodules (Fig. S2).

In order to determine the structure of the *SymCRK* (Medtr3g079850.1) gene in the R108 background, the corresponding cDNA was cloned and sequenced. The gene harbors six introns and seven exons (Fig. 1a) and corresponds to the Affymetrix Microarray probe sets, Mtr.39654.1.S1_at and Mtr.44507.1.S1_at (Table S1, Fig. S1). In the mutant line NF0737, the *Tnt1* insertion is located in the third exon (Fig. 1a). The gene encodes for a protein of 654 amino acid residues. Analysis of the primary sequence of the protein using the SMART server (http://smart.embl-heidelberg.de/; Schultz *et al.*, 1998; Letunic *et al.*, 2012) indicates that the predicted protein harbors a signal peptide, two extracellular cysteine-rich domains of unknown function 26 (DUF26), a transmembrane domain and a serine/threonine protein kinase domain (Fig. 1b), and thus belongs to the family of cysteine-rich kinases (CRKs; Chen, 2001). Interestingly, Mt_SymCRK contains a nonRD motif in the activation loop of the protein kinase domain (Figs 1b, S3) that is typical of pattern recognition receptors (PRRs) involved in plant and animal innate immunity (Dardick & Ronald, 2006; Dardick *et al.*, 2012). A careful analysis of the predicted protein database indicates that nonRD CRKs are only found in legume plants (one in *M. truncatula*, one in *Lotus japonicus* (chr6.CM0041.530.r2.a) and one in *Cicer arietinum* (XP_004502136.1)). By contrast, the 41 *Arabidopsis* CRKs are RD kinases (Fig. S3). Despite the presence of a nonRD motif, a phylogenetic analysis indicates that the kinase domains of these three nonRD CRKs of legumes are closer to RD CRK kinase domains than to nonRD kinase domains of PRRs such as At-FLS2 or AtEFR (Fig. S4). Interestingly, the occurrence of the nonRD motif in these three legume CRKs is correlated with an atypical motif in the N-terminal DUF26 domain (Fig. S3). Cysteine-rich RLK proteins contain two copies of C-X_8-C-X_2-C in the extracellular domains (DUF26; Chen, 2001). By contrast, Mt_SymCRK and its two legume homologs display a C-X_6-C-X_2-C motif in the N-terminal DUF26.

Mt_SymCRK is required for nitrogen fixation

Like the *dnf2* mutant, the *symCRK* mutant produces a mixture of white and necrotic nodules when grown on an agar-based substrate (Fig. 2d, Table S3). However, the proportion of necrotic nodules to white nodules was significantly higher in the *symCRK* than in the *dnf2* mutant (Fig. 2d). We previously observed that DNF2 is facultative for symbiosis *in vitro* when Phytagel was used instead of agar to solidify the medium (Berrabah *et al.*, 2014). In order to determine if *symCRK* also displays this conditional requirement, we grew and inoculated *M. truncatula* wild-type, *dnf2* and *symCRK* plants with *S. medicae*, *in vitro*, on medium solidified with agar or Phytagel, and evaluated the symbiotic capacity of the plants using the ARA. In contrast to *dnf2*, which displayed the conditional phenotype (i.e. fix^+ on Phytagel and fix^- on agar), *symCRK*-nodulated plants were unable to reduce acetylene on both substrates tested (Fig. 3). Together, our data support an essential role for *SymCRK* in nitrogen fixation.

SymCRK is required for normal nodule zonation

In order to get further insight into the role of *SymCRK* during symbiosis, histological analyses of the mutant nodules were performed. The initial steps of the symbiotic process were not altered in the *symCRK* mutant. Indeed, the mutant nodules displayed the typical elongated shape of indeterminate nodules, and symbiotic cells seemed to be correctly infected (Fig. 4). However, in *symCRK* nodules, zone III was drastically reduced compared

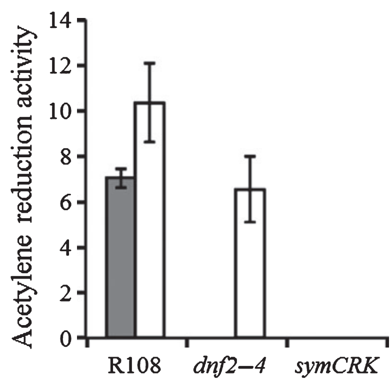

Fig. 3 *SymCRK* is required for nitrogen fixation. Acetylene reduction assay (ARA) reflecting nitrogenase activity was performed on nodulated *Medicago truncatula* plants cultivated on buffered nodulation medium solidified with agar (closed bars) or Phytagel (open bars). Nodulation was induced by *Sinorhizobium medicae* WSM419, and acetylene reduction activity per plant ($n = 3$) was measured 2 wk after inoculation. The ARA is expressed as nmole ethylene produced h^{-1} per plant. Error bars, ± SE. This experiment has been reproduced with similar results.

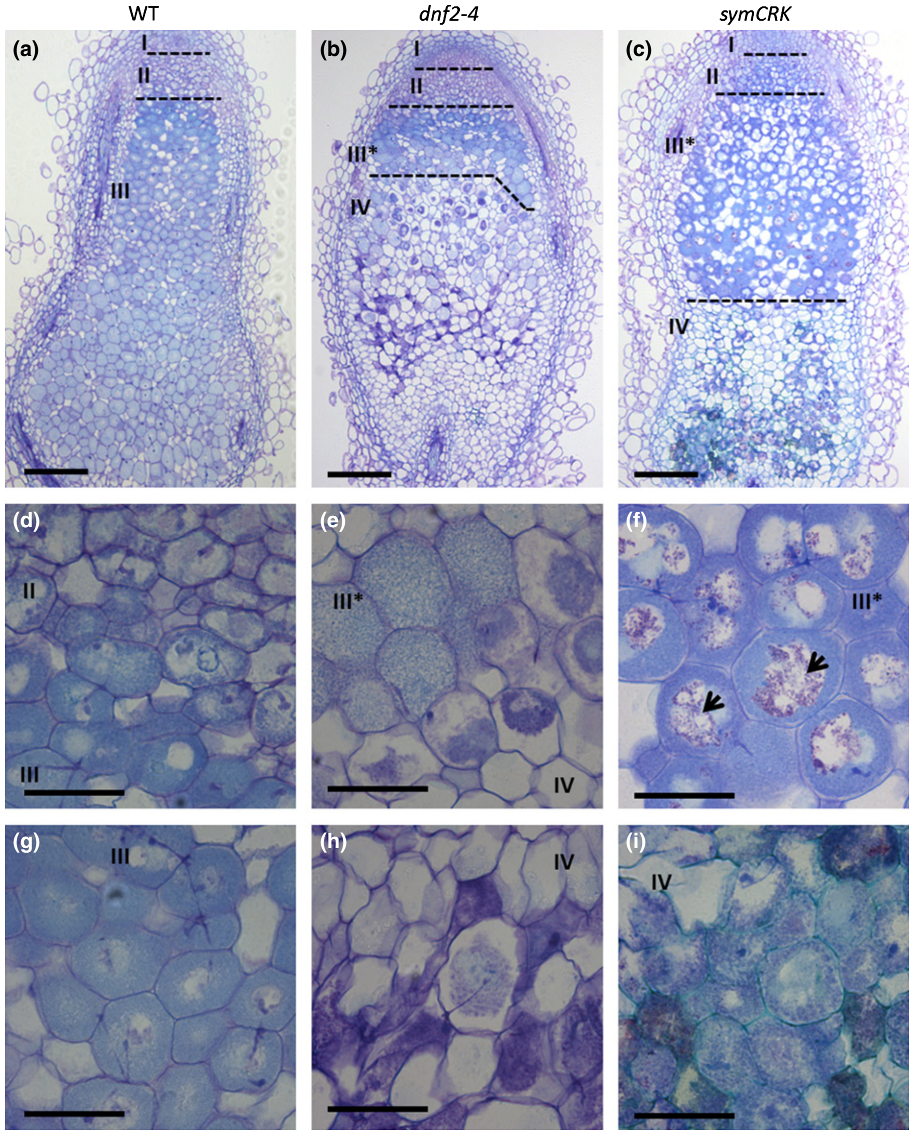

Fig. 4 *SymCRK* is required to prevent early senescence. Sections of *Medicago truncatula* wild-type (WT; a, d, g), *dnf2* (b, e, h), and *symCRK* (c, f, i) nodules 38 d after inoculation with *Sinorhizobium meliloti* strain Rm41. Meristematic (I), infection (II), fixation (III or III*) and senescent (IV) zones are delimited in panels (a)–(c) by dashed lines. (d–i) These represent enlargement of (a)–(c) in the indicated zones (roman numbers on the pictures). Nodule sections were stained using toluidine blue. Arrows in (f) indicate the degraded material in the vacuole. The material deposited between cells and staining darker in (h) and (i) may represent phenolics. Bars: (a–c) 200 μm; (d–i) 50 μm.

with the wild-type nodules and a senescent zone with plant cells devoid of bacteria was observed. Comparison with *dnf2* nodule sections revealed that the modification of the nodule zonation is less severe in the *symCRK* mutant than in the *dnf2* mutant in which zone III is smaller and zone IV is larger than in wild-type plants. This observation was further confirmed by comparisons of the endoreduplication indexes (EI) determined using flow cytometry analysis of the nodule nuclei (Fig. S5, Table S4). The EI was higher in the *symCRK* than in *dnf2* (Fig. S5, Table S4). In addition, in the *symCRK* nodules, degradation of material was observed in the vacuoles of infected cells (Fig. 4f).

SymCRK is required for bacteroids differentiation

Bacteroid differentiation in *symCRK* was evaluated by flow cytometry analysis (Fig. 5A). For this experiment, the *Sinorhizobium meliloti* strain Sm1021 was used together with its derivative mutant *bacA*, which is unable to undergo terminal bacteroid differentiation (Glazebrook *et al.*, 1993). A *bacA* mutant does not exist in another rhizobium strain that can efficiently nodulate *M. truncatula* R108. The DNA content of the bacteroids extracted from *dnf2* and *symCRK* nodules induced by wild-type *S. meliloti* (Sm1021) were similar to bacteroids prepared from wild-type *M. truncatula* R108 plants infected by the *S. meliloti bacA* mutant (Fig. 5A). In agreement with this observation, analysis of confocal microscopy images revealed that the bacteroids in *symCRK* and *dnf2* mutants were smaller than those in the wild-type *M. truncatula* plants (Fig. 5B). Wild-type, *dnf2* and *symCRK* bacteroids had average sizes of 7, 3 and 1.5 μm, respectively. Bacteroids of the *bacA* mutant on wild-type plants had the same size as *symCRK* bacteroids (Fig. 5B).

As mentioned earlier, in *M. truncatula*, terminal differentiation of bacteroid is triggered by NCR peptides. In order to determine if the lack of bacteroid differentiation observed in *symCRK* is correlated with reduced NCR production, expression of six genes encoding NCR peptides was investigated by RT-qPCR in nodules of *M. truncatula* (R108) wild-type, *symCRK*, *dnf2* and in *bacA*-induced nodules (Fig. 5C). Expression of the early NCR

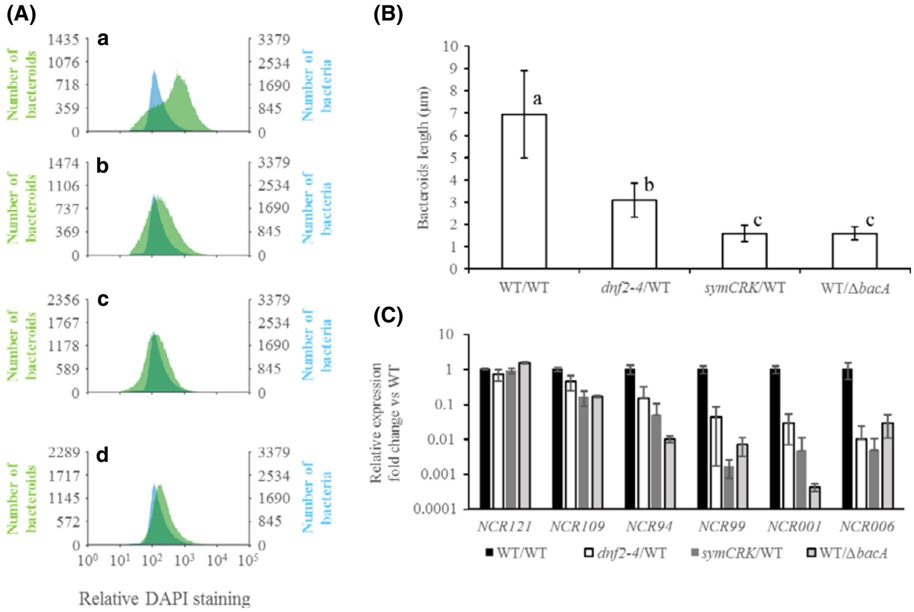

Fig. 5 *SymCRK* is required for bacteroid differentiation. (A) Flow cytometry analysis of 4′,6′-diamidino-2-phenylindol (DAPI)-stained bacteroids extracted from *Medicago truncatula* wild-type (WT; a, d), *dnf2* (b) and *symCRK* plants (c) 35 d after inoculation with *Sinorhizobium meliloti* Sm1021 (a– c) or with the Sm1021 *bacA* mutant (d). Results obtained with isolated bacteroids and free-living bacteria are represented in green and in blue, respectively. On these diagrams, the *y*-axis represents the numbers of counted objects, and the *x*-axis represents DAPI fluorescence measurements on a log scale (reflecting the DNA contents). (B) Bacteroid size determined by image analysis: wild-type, *dnf2* and *symCRK* bacteroids are an average of 7, 3 and 1.5 µm long, respectively. *symCRK* bacteroids display the same size as the *bacA* mutant and free-living bacteria (1.5 µm). Error bars, ± SD from 60 measurements. A parametrical one-way ANOVA test (*P*-value < 2.2e–16) and a *post hoc* Tukey–Kramer test (95%) were performed, and statistically identical values are attributed with identical letters (*n* = 60). (C) *NCR* gene expression was evaluated by reverse transcription quantitative polymerase chain reaction (RT-qPCR) in the indicated nodules 14 d after inoculation with Sm1021 or Sm1021 *bacA*. Fold change vs WT is presented after normalization with an *Actin* gene as an internal control. Error bars, ± SE from two technical replicates from two independent experiments. Expression of late nodule-specific cysteine-rich (NCR) peptides is altered in the defective nodules.

peptide encoding gene *NCR121* (MtGEA) was not altered in any of the tested nodules. By contrast, expression of later NCR peptide encoding *NCR* genes (*NCR094*, *NCR099*, *NCR001*, *NCR006* and *NCR109*; MtGEA) was drastically reduced in nodules of the *symCRK* and *dnf2* mutants, as well as in the nodules induced by the *bacA* mutant in wild-type plants. Interestingly, *NCR109* and *NCR094*, whose expression is induced earlier than *NCR099*, *NCR001* and *NCR006* during the symbiotic process, were less reduced (Fig. 5C). These data indicate that, similar to that of *dnf2* mutant, *symCRK* bacteroids are altered in the differentiation process and that this alteration is correlated with a defect in *NCR* expression.

SYMCRK is required to repress defense-like reactions in nodules

In a previous study, *DNF2* was shown to be required to prevent phenolics accumulation and nodule necrosis and to repress defense-related gene expression (Bourcy *et al.*, 2013b; Berrabah *et al.*, 2014). In order to determine if *SymCRK* also prevents defense-like reactions in the nodules, accumulation of phenolic compounds was investigated in the nodules formed by the *symCRK* mutant by staining nodule sections with $KMnO_4$/methylene blue (Vasse *et al.*, 1993). Fig. 6(A) represents fixed nodule sections. Phenolics are revealed by blue pigmentation in panels (b), (d) and (f). The brown pigmentation observed in images (b), (d), and (f) correspond to $KMnO_4$ residues. Similar to *dnf2* nodules, *symCRK* displayed accumulation of phenolics at the base of the nodules induced by both *S. medicae* and *S. meliloti* (Figs 6A (c)–(f), S6). In necrotic nodules, accumulation of phenolics colocalized with necrosis. In order to investigate the expression of defense gene markers, RT-qPCR experiments were performed using RNAs extracted from wild-type, *dnf2* and *symCRK* nodules induced by both *S. medicae* and *S. meliloti*. The expression of six defense gene markers, that is, the *PR10* gene (Samac *et al.*, 2011), chitinase (Nars *et al.*, 2013), vegetative storage protein (*VSP*), phenylalanine ammonia lyase (*PAL*), β-endoglucanase (*BGL*; Gao *et al.*, 2007) and nondisease resistance 1 (*NDR1*; Century *et al.*, 1997), was evaluated. In the nodules of both *dnf2* and *symCRK*, expressions of all the six defense genes tested were stronger than in the wild-type inoculated with *S. medicae* or *S. meliloti* (Figs 6B and S6, respectively). The viability of the bacteroids in the wild-type, *dnf2* and *symCRK* nodules was also evaluated with the life-dead staining procedure that stains either green or red for living or dead bacteria, respectively (Haag *et al.*, 2011). In agreement with the defense-like reactions observed in nodules of the two mutants, bacteroid viability was altered as compared with the wild-type. However, in contrast to *dnf2* in which all bacteria were dead in zone III, *symCRK* zone III displayed a mixture of dead and live bacteroids (Fig. 6C).

Thus, taken together, the accumulation of defense-like phenolic compounds, the induction of defense marker genes and the

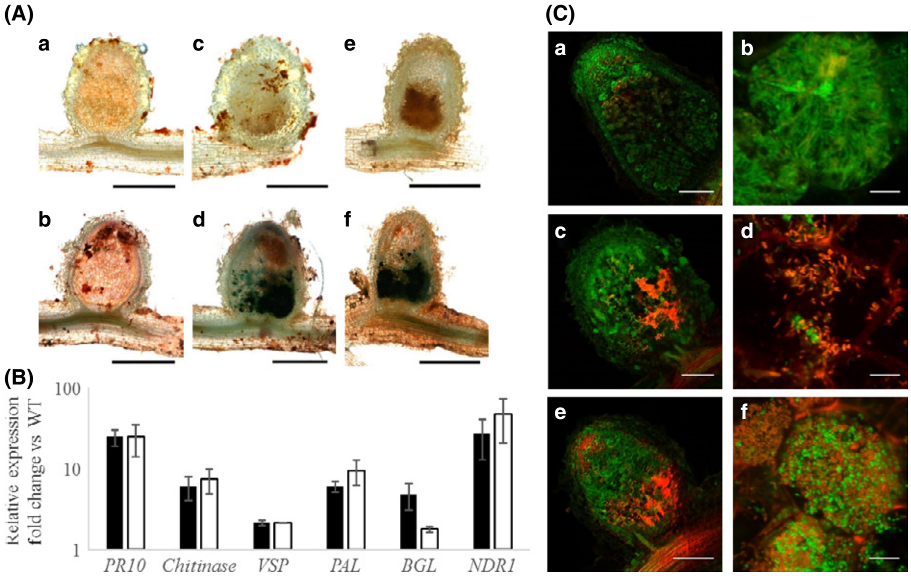

Fig. 6 *SymCRK* is required to prevent defense-like reactions in nodules. (A) Wild-type (WT; a, b), *dnf2* (c, d), and *symCRK* (e, f) *Medicago truncatula* nodule sections with (b, d, f) or without (a, c, e) $KMnO_4$/methylene blue staining reveal the presence of phenolic compounds in *dnf2* (d) and *symCRK* (f) nodules observed 21 d after inoculation (dai) with *Sinorhizobium medicae* WSM419 strain. Bars, 500 μm. (B) Expression of defense-related genes is induced in *dnf2* (black bars) and *symCRK* (white bars) nodules as compared with the wild-type. Reverse transcription quantitative polymerase chain reaction (RT-qPCR) was performed on RNAs extracted from nodules 21 dai with *S. medicae* WSM419. Fold change vs WT is presented after normalization with an *Actin* gene as an internal control. Error bars, ± SE from two independent experiments with two technical replicates for each experiment. (C) The bacteroid viability is altered in nodules of *symCRK* and *dnf2* mutants. Bacterial viability was evaluated in WT (a, b), *dnf2* (c, d) and *symCRK* (e, f) nodules 21 dai with *S. meliloti* 1021 using live/dead staining; live and dead bacteria are stained green and red, respectively. Bars: (a, c, e) 200 μm; (b, d, f) 20 μm.

partial mortality of the bacteroids suggest that, similar to *DNF2*, the *SymCRK* gene is required to repress defense-like reactions during the symbiotic process.

Discussion

By using genomics resources available for *M. truncatula* (Benedito *et al.*, 2008; He *et al.*, 2009; Cheng *et al.*, 2011), we identified a gene required for nitrogen fixation, bacteroid differentiation, preventing nodule early senescense, and preventing defense-like reactions in nodules. This gene is expressed specifically during the symbiotic process and encodes a receptor-like kinase of the cystein rich superfamilly. Interestingly, a close homolog of *SymCRK* is present in the *L. japonicus* genome and is also specifically expressed in nodules (Verdier *et al.*, 2013), suggesting a common function for these genes.

Cysteine-rich kinase family members generally harbor two extracellular cystein-rich motifs (Chen, 2001) of unknown function (the DUF26 domains). Little is known about this superfamily, but in *Arabidopsis*, some members were identified as being up-regulated upon treatment with the defense-related phytohormone salicylic acid (SA) or after inoculation with the phytopathogenic bacteria *Pseudomonas syringae* pv. tomato strain DC3000 (Du & Chen, 2000). The transcriptional behavior of the complete superfamily of CRK has been studied in *Arabidopsis* and transcription of some members is induced upon treatment with H_2O_2, the plant immunity activator peptide flg22, SA, and O_3 (Wrzaczek *et al.*, 2010), thus suggesting a role for these receptors in plant immunity.

A few functional studies support a role for the CRK members in plant immunity: in *Arabidopsis*, overexpression of either *CRK5* or *CRK13* enhanced resistance against *P. syringae* pv. tomato strain DC3000 (Chen *et al.*, 2003; Acharya *et al.*, 2007). Such a positive effect of CRK on plants challenged by a pathogenic organism is not a general feature of CRK as the loss of function of *CRK20* in *Arabidopsis* also results in increased resistance to *P. syringae* pv. tomato strain DC3000 (Ederli *et al.*, 2011). Similar to *CRK20*, transient gene silencing of *HvCRK1* in barley (*Hordeum vulgare*) triggers an enhanced resistance against the biotrophic fungus *Blumeria graminis* (the causal agent of powdery mildew; Rayapuram *et al.*, 2012). The authors suggested that *HvCRK1* is involved in the negative regulation of basal resistance. In nodules, the negative effect of *SymCRK* on plant defense-like reactions resembles the phenotypes of *HvCRK1* silencing and *Arabidopsis crk20* mutant. However, sequence relationships between these CRK members do not correlate with the suggested functions. For example, At_CRK20 and At_CRK5 cluster in the same group (Figs S4, S7).

Interestingly, the DUF26 domain is not restricted to CRKs and is also present in nonkinase proteins. Amongst these is the ginkbilobin -2, a protein accumulated in *Ginkgo biloba* seeds that displays antifungal activity (Sawano *et al.*, 2007). The structure of ginkbilobin-2 has been resolved (Miyakawa *et al.*, 2007), but the molecular basis of its antifungal activity remains unknown. Proteins containing DUF26 domains were also associated with other plant–fungus interactions. Upon infection with the phytopathogenic fungus *Magnaporthe oryzae*, secreted DUF26 containing proteins are more abundant in intercellular washing fluids of rice (Shenton *et al.*, 2012). All these data suggest a functional link between DUF26-containing proteins and phytopathogenic interactions. However, the role of DUF26 might not be restricted to biotic stress responses. Indeed, reduction of *CRK36* expression by RNAi in *Arabidopsis* triggers a higher sensitivity to the stress hormone ABA and to osmotic stress during the post-germination growth phase (Tanaka *et al.*, 2012). This suggests that the CRK family might be involved in response to both biotic and abiotic stresses.

An intriguing feature of SymCRK is the presence of a nonRD motif in the activation loop of the protein kinase domain. Association of a nonRD motif to this class of receptor kinases is specific to legumes. In plants and animals, the nonRD motif is associated with PRR (Dardick & Ronald, 2006; Dardick *et al.*, 2012; Schwessinger & Ronald, 2012) perceiving microbial invaders and triggering pattern-triggered immunity (PTI) (Zipfel, 2008; Boller & Felix, 2009; Segonzac & Zipfel, 2011). In this context, it is interesting to note the presence of a signal peptide and the expression of *SymCRK* in zones II and III (Roux *et al.*, 2014) of the nodules. These together suggest that SymCRK could be localized to the symbiosome membrane so that the extracellular DUF26 domains might be in close vicinity with the bacteroids. Considering the induction of defense-like reactions in nodules of the *symCRK* mutant, it is thus tempting to speculate that during evolution legumes coopted defense perception elements to build a molecular mechanism preventing the elimination of the symbiont.

Influence of innate immunity during rhizobia/legume symbioses has been studied previously, notably in *Lotus* and *Medicago*. These studies indicated that both SA, the defense-related phytohormone (Stacey *et al.*, 2006), and Flg22, a PTI elicitor (Lopez-Gomez *et al.*, 2012), have a negative impact on the early steps of the symbiotic process. In addition, transcriptome analysis indicates that defenses can be elicited during the first step of the symbiosis, but that bacterial exopolysaccharides repress the development of the plant defenses (Jones *et al.*, 2008). Nodulation factors, produced by rhizobia, are also able to suppress immunity triggered by microbial-associated molecular pattern on soybean as well as on nonlegume plants, such as corn, tomato and *Arabidopsis* (Liang *et al.*, 2013). These data, as well as other recent studies (Scheidle *et al.*, 2005; Yang *et al.*, 2010; Okazaki *et al.*, 2013; Rey *et al.*, 2013), suggest a major role for immunity modulation in the successful establishment of the symbiotic process. However, these studies did not address the role of immunity in the later steps of the symbiosis (chronic infection), which is reported in this manuscript.

What triggers defense-like reactions in *dnf2* and *symCRK* nodules remains to be elucidated. Despite similarities between the two mutants, *symCRK* does not have the conditional phenotype observed for *dnf2*. Furthermore, in the *dnf2* nodules, the infected zone is smaller and the symbiotic cells are less well differentiated than in the *symCRK* mutant, and in addition bacteroid loss of viability is higher in the *dnf2* nodules. All these differences suggest that two similar but distinct pathways can activate plant defense-like reactions in the nodule and the action of only one, repressed by DNF2, depends on the environmental conditions. The second one is repressed by SymCRK, and whether the two pathways are independent or converge should be the focus of future studies and will require the analyses of the *dnf2 symCRK* double mutant.

Acknowledgements

We are grateful to Samuel Mondy for statistical analyses and Stephanie Pedrosa for technical assistance. This work was supported by the Centre National de la Recherche Scientifique (CNRS) and a grant Agence Nationale de la Recherche (ANR) Blanc International SVSE 6.2010.1 (LEGUMICS) to P.R. M.B. was supported by a PhD fellowship from the French Ministry of Research. This work has benefited from a French state grant (reference ANR-10-LABX-0040-SPS) managed by the French National Research Agency under an Investments for the Future program (reference no ANR-11-IDEX-0003-02). This work has benefited from the facilities and expertise of the IMAGIF Cell Biology Unit of the Gif campus (www.imagif.cnrs.fr), which is supported by the Conseil Général de l'Essonne. *M. truncatula Tnt1* mutants used in this study were generated using funds from the Samuel Roberts Noble Foundation and National Science Foundation (award no. DBI 0703285).

References

Acharya BR, Raina S, Maqbool SB, Jagadeeswaran G, Mosher SL, Appel HM, Schultz JC, Klessig DF, Raina R. 2007. Overexpression of *crk13*, an *Arabidopsis* cysteine-rich receptor-like kinase, results in enhanced resistance to *Pseudomonas syringae*. *Plant Journal* **50**: 488–499.

Beatty PH, Good AG. 2011. Plant science. Future prospects for cereals that fix nitrogen. *Science* **333**: 416–417.

Benedito VA, Torres-Jerez I, Murray JD, Andriankaja A, Allen S, Kakar K, Wandrey M, Verdier J, Zuber H, Ott T *et al.* 2008. A gene expression atlas of the model legume *Medicago truncatula*. *Plant Journal* **55**: 504–513.

Berrabah F, Bourcy M, Cayrel A, Eschstruth A, Mondy S, Ratet P, Gourion B. 2014. Growth conditions determine the *dnf2* requirement for symbiosis. *PLoS ONE* **9**: e91866.

Boisson-Dernier A, Chabaud M, Garcia F, Becard G, Rosenberg C, Barker DG. 2001. *Agrobacterium rhizogenes*-transformed roots of *Medicago truncatula* for the study of nitrogen-fixing and endomycorrhizal symbiotic associations. *Molecular Plant Microbe Interactions* **14**: 695–700.

Boller T, Felix G. 2009. A renaissance of elicitors: perception of microbe-associated molecular patterns and danger signals by pattern-recognition receptors. *Annual Review of Plant Biology* **60**: 379–406.

Bourcy M, Berrabah F, Ratet P, Gourion B. 2013a. Failure of self-control: defense-like reactions during legume/rhizobia symbiosis. *Plant Signaling & Behavior* **8**: e23915.

Bourcy M, Brocard L, Pislariu CI, Cosson V, Mergaert P, Tadege M, Mysore KS, Udvardi MK, Gourion B, Ratet P. 2013b. *Medicago truncatula* DNF2 is a PI-PLC-XD-containing protein required for bacteroid persistence and prevention of nodule early senescence and defense-like reactions. *New Phytologist* **197**: 1250–1261.

Century KS, Shapiro AD, Repetti PP, Dahlbeck D, Holub E, Staskawicz BJ. 1997. Ndr1, a pathogen-induced component required for *Arabidopsis* disease resistance. *Science* **278**: 1963–1965.

Charpentier M, Oldroyd G. 2010. How close are we to nitrogen-fixing cereals? *Current Opinion in Plant Biology* **13**: 556–564.

Chen K, Du L, Chen Z. 2003. Sensitization of defense responses and activation of programmed cell death by a pathogen-induced receptor-like protein kinase in *Arabidopsis*. *Plant Molecular Biology* **53**: 61–74.

Chen Z. 2001. A superfamily of proteins with novel cysteine-rich repeats. *Plant Physiology* **126**: 473–476.

Cheng X, Wang M, Lee HK, Tadege M, Ratet P, Udvardi M, Mysore KS, Wen J. 2013. An efficient reverse genetics platform in the model legume *Medicago truncatula*. *New Phytologist* **201**: 1065–1076.

Cheng X, Wen J, Tadege M, Ratet P, Mysore KS. 2011. Reverse genetics in *Medicago truncatula* using *Tnt1* insertion mutants. *Methods in Molecular Biology* **678**: 179–190.

Dardick C, Ronald P. 2006. Plant and animal pathogen recognition receptors signal through non-rd kinases. *PLoS Pathogens* **2**: e2.

Dardick C, Schwessinger B, Ronald P. 2012. Non-arginine-aspartate (non-RD) kinases are associated with innate immune receptors that recognize conserved microbial signatures. *Current Opinion in Plant Biology* **15**: 358–366.

Du L, Chen Z. 2000. Identification of genes encoding receptor-like protein kinases as possible targets of pathogen- and salicylic acid-induced WRKY DNA-binding proteins in *Arabidopsis*. *Plant Journal* **24**: 837–847.

Ederli L, Madeo L, Calderini O, Gehring C, Moretti C, Buonaurio R, Paolocci F, Pasqualini S. 2011. The *Arabidopsis thaliana* cysteine-rich receptor-like kinase CRK20 modulates host responses to *Pseudomonas syringae pv.* Tomato DC3000 infection. *Journal of Plant Physiology* **168**: 1784–1794.

Ehrhardt DW, Atkinson EM, Long SR. 1992. Depolarization of alfalfa root hair membrane potential by *Rhizobium meliloti* nod factors. *Science* **256**: 998–1000.

Ferguson GP, Roop RM 2nd, Walker GC. 2002. Deficiency of a *Sinorhizobium meliloti bacA* mutant in alfalfa symbiosis correlates with alteration of the cell envelope. *Journal of Bacteriology* **184**: 5625–5632.

Galibert F, Finan TM, Long SR, Puhler A, Abola P, Ampe F, Barloy-Hubler F, Barnett MJ, Becker A, Boistard P *et al.* 2001. The composite genome of the legume symbiont *Sinorhizobium meliloti*. *Science* **293**: 668–672.

Gao LL, Anderson JP, Klingler JP, Nair RM, Edwards OR, Singh KB. 2007. Involvement of the octadecanoid pathway in blue green aphid resistance in *Medicago truncatula*. *Molecular Plant Microbe Interactions* **20**: 82–93.

Glazebrook J, Ichige A, Walker GC. 1993. A *Rhizobium meliloti* homolog of the *Escherichia coli* peptide-antibiotic transport protein SbmA is essential for bacteroid development. *Genes & Development* **7**: 1485–1497.

Haag AF, Baloban M, Sani M, Kerscher B, Pierre O, Farkas A, Longhi R, Boncompagni E, Herouart D, Dall'angelo S *et al.* 2011. Protection of *Sinorhizobium* against host cysteine-rich antimicrobial peptides is critical for symbiosis. *PLoS Biology* **9**: e1001169.

He J, Benedito VA, Wang M, Murray JD, Zhao PX, Tang Y, Udvardi MK. 2009. The *Medicago truncatula* gene expression atlas web server. *BMC Bioinformatics* **10**: 441.

Hoffmann B, Trinh TH, Leung J, Kondorosi A, Kondorosi E. 1997. A new *Medicago truncatula* line with superior *in vitro* regeneration, transformation, and symbiotic properties isolated through cell culture selection. *Molecular Plant Microbe Interactions* **10**: 307–315.

Howieson J, Ewing M. 1986. Acid tolerance in the *Rhizobium meliloti–Medicago* symbiosis. *Australian Journal of Agricultural Research* **37**: 55–64.

Iantcheva A, Chabaud M, Cosson V, Barascud M, Schutz B, Primard-Brisset C, Durand P, Barker DG, Vlahova M, Ratet P. 2009. Osmotic shock improves *Tnt1* transposition frequency in *Medicago truncatula* cv jemalong during *in vitro* regeneration. *Plant Cell Reports* **28**: 1563–1572.

Jones KM, Sharopova N, Lohar DP, Zhang JQ, VandenBosch KA, Walker GC. 2008. Differential response of the plant *Medicago truncatula* to its symbiont *Sinorhizobium meliloti* or an exopolysaccharide-deficient mutant. *Proceedings of the National Academy of Sciences, USA* **105**: 704–709.

Koch B, Evans HJ. 1966. Reduction of acetylene to ethylene by soybean root nodules. *Plant Physiology* **41**: 1748–1750.

Kondorosi E, Banfalvi Z, Kondorosi A. 1984. Physical and genetic analysis of a symbiotic region of *Rhizobium meliloti*: identification of nodulation genes. *Molecular and General Genetics* **193**: 445–452.

Kondorosi E, Mergaert P, Kereszt A. 2013. A paradigm for endosymbiotic life: cell differentiation of *Rhizobium* bacteria provoked by host plant factors. *Annual Review of Microbiology* **67**: 611–628.

Krall L, Wiedemann U, Unsin G, Weiss S, Domke N, Baron C. 2002. Detergent extraction identifies different VirB protein subassemblies of the type IV secretion machinery in the membranes of *Agrobacterium tumefaciens*. *Proceedings of the National Academy of Sciences, USA* **99**: 11405–11410.

Letunic I, Doerks T, Bork P. 2012. Smart 7: recent updates to the protein domain annotation resource. *Nucleic Acids Research* **40**: D302–D305.

Liang Y, Cao Y, Tanaka K, Thibivilliers S, Wan J, Choi J, Kang C, Qiu J, Stacey G. 2013. Nonlegumes respond to rhizobial nod factors by suppressing the innate immune response. *Science* **341**: 1384–1387.

Lopez-Gomez M, Sandal N, Stougaard J, Boller T. 2012. Interplay of flg22-induced defence responses and nodulation in *Lotus japonicus*. *Journal of Experimental Botany* **63**: 393–401.

Maunoury N, Redondo-Nieto M, Bourcy M, Van de Velde W, Alunni B, Laporte P, Durand P, Agier N, Marisa L, Vaubert D *et al.* 2010. Differentiation of symbiotic cells and endosymbionts in *Medicago truncatula* nodulation are coupled to two transcriptome-switches. *PLoS ONE* **5**: e9519.

Mergaert P, Uchiumi T, Alunni B, Evanno G, Cheron A, Catrice O, Mausset AE, Barloy-Hubler F, Galibert F, Kondorosi A *et al.* 2006. Eukaryotic control on bacterial cell cycle and differentiation in the *Rhizobium*–legume symbiosis. *Proceedings of the National Academy of Sciences, USA* **103**: 5230–5235.

Miyakawa T, Sawano Y, Miyazono K, Hatano K, Tanokura M. 2007. Crystallization and preliminary X-ray analysis of ginkbilobin-2 from *Ginkgo biloba* seeds: a novel antifungal protein with homology to the extracellular domain of plant cysteine-rich receptor-like kinases. *Acta Crystallographica Section F, Structural Biology and Crystallization Communications* **63**: 737–739.

Nars A, Rey T, Lafitte C, Vergnes S, Amatya S, Jacquet C, Dumas B, Thibaudeau C, Heux L, Bottin A *et al.* 2013. An experimental system to study responses of *Medicago truncatula* roots to chitin oligomers of high degree of polymerization and other microbial elicitors. *Plant Cell Reports* **32**: 489–502.

Okazaki S, Kaneko T, Sato S, Saeki K. 2013. Hijacking of leguminous nodulation signaling by the rhizobial type III secretion system. *Proceedings of the National Academy of Sciences, USA* **110**: 17131–17136.

Oldroyd GE, Murray JD, Poole PS, Downie JA. 2011. The rules of engagement in the legume–rhizobial symbiosis. *Annual Review of Genetics* **45**: 119–144.

Pislariu CI, Murray JD, Wen J, Cosson V, Muni RR, Wang M, Benedito VA, Andriankaja A, Cheng X, Jerez IT *et al.* 2012. A *Medicago truncatula* tobacco retrotransposon insertion mutant collection with defects in nodule development and symbiotic nitrogen fixation. *Plant Physiology* **159**: 1686–1699.

Rayapuram C, Jensen MK, Maiser F, Shanir JV, Hornshoj H, Rung JH, Gregersen PL, Schweizer P, Collinge DB, Lyngkjaer MF. 2012. Regulation of basal resistance by a powdery mildew-induced cysteine-rich receptor-like protein kinase in barley. *Molecular Plant Pathology* **13**: 135–147.

Rey T, Nars A, Bonhomme M, Bottin A, Huguet S, Balzergue S, Jardinaud MF, Bono JJ, Cullimore J, Dumas B *et al.* 2013. Nfp, a lysM protein controlling nod factor perception, also intervenes in *Medicago truncatula* resistance to pathogens. *New Phytologist* **198**: 875–886.

Rosenberg C, Boistard P, Denarie J, Casse-Delbart F. 1981. Genes controlling early and late functions in symbiosis are located on a megaplasmid in *Rhizobium meliloti*. *Molecular and General Genetics* **184**: 326–333.

Roux B, Rodde N, Jardinaud MF, Timmers T, Sauviac L, Cottret L, Carrere S, Sallet E, Courcelle E, Moreau S *et al.* 2014. An integrated analysis of plant and bacterial gene expression in symbiotic root nodules using laser capture microdissection coupled to rna-seq. *Plant Journal* **77**: 817–837.

Samac DA, Penuela S, Schnurr JA, Hunt EN, Foster-Hartnett D, Vandenbosch KA, Gantt JS. 2011. Expression of coordinately regulated defence response genes and analysis of their role in disease resistance in *Medicago truncatula*. *Molecular Plant Pathology* **12**: 786–798.

Sawano Y, Miyakawa T, Yamazaki H, Tanokura M, Hatano K. 2007. Purification, characterization, and molecular gene cloning of an antifungal protein from *Ginkgo biloba* seeds. *Biological Chemistry* **388**: 273–280.

Scheidle H, Gross A, Niehaus K. 2005. The lipid a substructure of the *Sinorhizobium meliloti* lipopolysaccharides is sufficient to suppress the oxidative burst in host plants. *New Phytologist* **165**: 559–565.

Schultz J, Milpetz F, Bork P, Ponting CP. 1998. Smart, a simple modular architecture research tool: identification of signaling domains. *Proceedings of the National Academy of Sciences, USA* **95**: 5857–5864.

Schwessinger B, Ronald PC. 2012. Plant innate immunity: perception of conserved microbial signatures. *Annual Review of Plant Biology* **63**: 451–482.

Segonzac C, Zipfel C. 2011. Activation of plant pattern-recognition receptors by bacteria. *Current Opinion in Microbiology* **14**: 54–61.

Shenton MR, Berberich T, Kamo M, Yamashita T, Taira H, Terauchi R. 2012. Use of intercellular washing fluid to investigate the secreted proteome of the rice-*Magnaporthe* interaction. *Journal of Plant Research* **125**: 311–316.

Stacey G, McAlvin CB, Kim SY, Olivares J, Soto MJ. 2006. Effects of endogenous salicylic acid on nodulation in the model legumes *Lotus japonicus* and *Medicago truncatula*. *Plant Physiology* **141**: 1473–1481.
Tadege M, Wen J, He J, Tu H, Kwak Y, Eschstruth A, Cayrel A, Endre G, Zhao PX, Chabaud M *et al.* 2008. Large-scale insertional mutagenesis using the *Tnt1* retrotransposon in the model legume *Medicago truncatula*. *Plant Journal* **54**: 335–347.
Tanaka H, Osakabe Y, Katsura S, Mizuno S, Maruyama K, Kusakabe K, Mizoi J, Shinozaki K, Yamaguchi-Shinozaki K. 2012. Abiotic stress-inducible receptor-like kinases negatively control ABA signaling in *Arabidopsis*. *Plant Journal* **70**: 599–613.
Udvardi M, Poole PS. 2013. Transport and metabolism in legume–rhizobia symbioses. *Annual Review of Plant Biology* **64**: 781–805.
Van de Velde W, Guerra JC, De Keyser A, De Rycke R, Rombauts S, Maunoury N, Mergaert P, Kondorosi E, Holsters M, Goormachtig S. 2006. Aging in legume symbiosis. A molecular view on nodule senescence in *Medicago truncatula*. *Plant Physiology* **141**: 711–720.
Van de Velde W, Zehirov G, Szatmari A, Debreczeny M, Ishihara H, Kevei Z, Farkas A, Mikulass K, Nagy A, Tiricz H *et al.* 2010. Plant peptides govern terminal differentiation of bacteria in symbiosis. *Science* **327**: 1122–1126.
Vasse J, de Billy F, Camut S, Truchet G. 1990. Correlation between ultrastructural differentiation of bacteroids and nitrogen fixation in alfalfa nodules. *Journal of Bacteriology* **172**: 4295–4306.
Vasse J, de Billy F, Truchet G. 1993. Abortion of infection during the *Rhizobium meliloti*–alfalfa symbiotic interaction is accompanied by a hypersensitive reaction. *Plant Journal* **4**: 555–566.
Verdier J, Torres-Jerez I, Wang M, Andriankaja A, Allen SN, He J, Tang Y, Murray JD, Udvardi MK. 2013. Establishment of the *Lotus japonicus* gene expression atlas (LjGEA) and its use to explore legume seed maturation. *Plant Journal* **74**: 351–362.
Wrzaczek M, Brosche M, Salojarvi J, Kangasjarvi S, Idanheimo N, Mersmann S, Robatzek S, Karpinski S, Karpinska B, Kangasjarvi J. 2010. Transcriptional regulation of the CRK/DUF26 group of receptor-like protein kinases by ozone and plant hormones in *Arabidopsis*. *BMC Plant Biology* **10**: 95.
Yang S, Tang F, Gao M, Krishnan HB, Zhu H. 2010. R gene-controlled host specificity in the legume-rhizobia symbiosis. *Proceedings of the National Academy of Sciences, USA* **107**: 18735–18740.
Young ND, Debelle F, Oldroyd GE, Geurts R, Cannon SB, Udvardi MK, Benedito VA, Mayer KF, Gouzy J, Schoof H *et al.* 2011. The *Medicago* genome provides insight into the evolution of rhizobial symbioses. *Nature* **480**: 520–524.
Zamioudis C, Pieterse CM. 2012. Modulation of host immunity by beneficial microbes. *Molecular Plant Microbe Interactions* **25**: 139–150.
Zipfel C. 2008. Pattern-recognition receptors in plant innate immunity. *Current Opinion in Immunology* **20**: 10–16.

Supporting Information

Additional supporting information may be found in the online version of this article.

Fig. S1 Expression profile of candidate genes.

Fig. S2 SymCRK expression is nodule-specific.

Fig. S3 SymCRK harbors atypical motifs in the DUF26 and kinase domains.

Fig. S4 SymCRK kinase domains are closer to RD-CRK kinases than to nonRD kinases.

Fig. S5 The *symCRK* endoreduplication index is higher than *dnf2*.

Fig. S6 Defense-like reactions in *dnf2* and *symCRK* nodules induced by strain Sm2011.

Fig. S7 Phylogenetic tree of DUF26.

Table S1 Candidate genes and corresponding mutant lines

Table S2 Primers used to evaluate genes expression by RT-qPCR

Table S3 Phenotype segregation analysis of the candidate mutant lines

Table S4 Endoreduplication levels of wild-type, *dnf2* and *symCRK* nodule cells

Please note: Wiley Blackwell are not responsible for the content or functionality of any supporting information supplied by the authors. Any queries (other than missing material) should be directed to the *New Phytologist* Central Office.